Iterative Modeling of Interior Ballistics of Small Arms

A. M. JOGLEKAR,* M. S. PHADKE,* S. M. WU†
University of Wisconsin, Madison, Wis.

Iterative model building technique is employed to develop an empirical-mechanistic interior ballistic model for 5.56 mm weapon using nitrocellulose propellant. The model is based upon one-dimensional fluid dynamic theory. A Lagrangean approach is used and a finite-difference scheme is presented for numerical solution of the pertinent partial differential equations. Experimentally observed chamber pressure-time curves are used for iterative improvements in the burning rate equation, which is the only unknown in the formulated model. The model is found to satisfactorily predict the observed pressure-time curves. A numerical evaluation of the model gives insight into the ballistic phenomena to be expected in practice and acts as a diagnostic check.

Nomenclature‡

A = bore cross sectional area
C = calorific value of propellant
C_p, C_v = specific heats of propellant gas at constant pressure, constant volume
E = specific energy of propellant gas
KE = kinetic energy of propellant and gas
K_1, K_2 = burning rate parameters
$\hat{K}_1, \hat{K}_2$ = estimated values of burning rate parameters
L, L_0 = scaled chamber and reference lengths
M_0 = total mass of propellant and gas in an element
M_g = mass of gas in an element
M_p = mass of propellant in an element
m = projectile mass
n_1 = total number of propellant particles
PE = potential (chemical) energy of propellant
P_o = reference pressure
p = pressure
p_a, p_b = pressures ahead of projectile and at projectile base
p_{min} = minimum starting pressure
Q = heat exchanged across the boundary of an element
R = displacement of an element from the breech end
R_0 = gas constant
R_b = displacement of the projectile from the breech end
r = instantaneous radius of propellant particles
S = burning surface area of a particle
SS = residual sum of squares
T = temperature
t = time
u, u_b = velocity, and projectile velocity
V_0 = reference specific volume
V_c = chamber volume
v = gaseous specific volume
W_1, W_2 = work done by the element and on the element
x = Lagrangean coordinate
γ = ratio of specific heats
η = specific covolume of propellant gas
ρ_0 = initial mass of propellant and air per unit chamber volume
ρ_1 = mass of propellant per unit volume of propellant
ρ_g, ρ_p = partial density of gas and propellant, respectively

Superscript

n = nth time step

Subscript

j = jth element boundary from breech end

Received May 17, 1972; revision received February 13, 1973. This work was supported, in part, by the U.S. Army Weapons Command under Contract DAAF0370C0073. The authors wish to thank J. Ramnarace and K. Thorson of the Olin Corporation, Badger Army Ammunition Plant, Baraboo, Wis. for conducting the experiments and for familiarizing the authors with the process of Ball Powder manufacture. The authors also wish to thank W. L. Dahl of the U.S. Army Weapons Command, Rock Island, Ill. for his interest in the project and for his comments on this paper. Use of the University of Wisconsin Computing Center was made possible through support, in part, from the National Science Foundation, other U.S. Government Agencies and the Wisconsin Alumni Research Foundation.

Index category: Multiphase Flows.

* Research Assistant, Department of Mechanical Engineering.
† Professor, Department of Mechanical Engineering, Department of Statistics.

‡ The quantities $E, KE, M_g, M_p, PE, p, R, r, S, t, u, v, W, \rho_g, \rho_p$ are functions of j and n. p_b, R_b, u_b are functions of n alone.

Introduction

CLASSICAL interior ballistic models were solely concerned with the development of pressure as determined by the burning law of propellant and the volume behind the projectile. Lagrange[1] first drew attention to the fluid dynamic aspects of interior ballistics. Since then, many investigators[2–6] have attempted analytical and numerical solutions for the Lagrange ballistic problem. Much of the work has been confined to the application of an assumed propellant burning rate to large caliber weapons using extruded propellant.

The objective of this paper is to introduce the iterative model building approach as a methodology to build an adequate interior ballistic model. A 5.56 mm weapon using nitrocellulose ammunition is considered. First, a model based upon one-dimensional Lagrangean fluid dynamic theory is formulated. An iterative scheme to improve the burning rate equation, which is the only unknown in the formulated model, is then presented. Finally, the model is numerically evaluated to gain a qualitative understanding of the interior ballistic phenomena to be expected in practice.

Lagrangean Fluid Dynamic Formulation

Lagrangean fluid dynamic equations governing the behavior of single phase flow, namely, the gaseous flow are well known.[7] These equations are directly applicable to the case of instantaneous burning of charge. In reality, the propellant continues to burn even after the projectile motion starts. Therefore, the flow consists of two phases: the propellant constitutes the solid phase and the gases of combustion constitute the gaseous phase. For this case of two phase flow, the governing hyperbolic partial differential equations and the corresponding difference equations are derived under the following set of assumptions: 1) The flow is one dimensional and laminar. 2) The chamber is replaced by a volumetrically equivalent tube of bore diameter. 3) Before ignition, propellant is uniformly distributed in the space behind the projectile.

During the projectile motion there is no relative motion between the propellant and the gas. 4) The gases of combustion are chemically inert, without viscosity or heat conduction. They obey the gas law $p(v-\eta)=R_0T$. The gases are polytropic with constant specific heats. Outside the zone of combustion, the entropy of gases remains constant. 5) The primary energy loss due to heat transfer and the secondary energy losses due to friction, gas leakages, projectile rotation, barrel strain, and recoil are neglected. 6) The engraving force is taken as a certain minimum starting pressure. Air pressure ahead of the projectile remains one atmosphere throughout the projectile motion. 7) The primer burns instantaneously. The corresponding generated pressure does not cause any projectile motion. 8) The entire charge ignites instantaneously after the primer energy is released. The charge is assumed to consist of identical spherical particles with constant specific gravity. The burning is assumed to proceed uniformly over the entire surface of the particles, without disrupting the one-dimensional flow.

Under these assumptions, the problem considered is as follows: There is an insulated tube of finite length and uniform diameter sealed at one end and open at the other end. Propellant forms the known energy, mass and volume source between the sealed end and the projectile. The resultant changes in the fluid properties, in the space behind the projectile, constitute the objects of solution to this problem.

Governing Equations for Two Phase Flow

The derivation of the necessary differential equations is based upon the state equation and the principles of conservation of mass, momentum and energy. To account for the transformation of the solid phase to the gaseous phase, a burning rate equation is necessary. These equations are to be solved for the specified initial and boundary conditions. Additionally, definitions of the velocity and the specific volume of gases are necessary.

Differential Equations

Referring to Fig. 1, the procedure to derive the differential equations is to first write the difference equations for the Lagrangean element $(x,x+\Delta x)$ and then take the appropriate limits. In the following, x and $x+\Delta x$ are denoted by j and $j+1$ whereas t and $t+\Delta t$ are represented by n and $n+1$.

Velocity Equation

$$(R_j^{n+1}-R_j^n)/\Delta t = u_j^{n+1/2} \tag{1}$$

Taking limit as $\Delta t \to 0$

$$\partial R/\partial t = u \tag{2}$$

Conservation of Mass

Equating mass in an element at time t to mass in the same element at $t=0$ leads to

$$M_{pj+1/2}{}^n + M_{gj+1/2}{}^n = M_0 \tag{3}$$

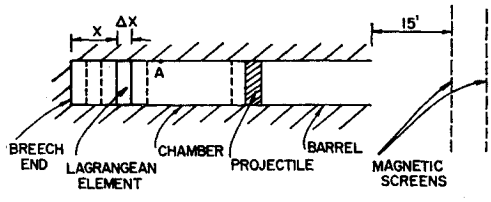

Fig. 1 Assumed weapon.

The mass of propellant and the mass of gas in an element are related to the propellant density and the gas density by

$$\left.\begin{aligned} M_{pj+1/2}{}^n &= \rho_{pj+1/2}{}^n \cdot (R_{j+1}{}^n - R_j{}^n)\cdot A \\ M_{gj+1/2}{}^n &= \rho_{gj+1/2}{}^n \cdot (R_{j+1}{}^n - R_j{}^n)\cdot A \end{aligned}\right\} \tag{4}$$

Substituting Eq. (4) in Eq. (3)

$$(\rho_{pj+1/2}{}^n + \rho_{gj+1/2}{}^n)\cdot(R_{j+1}{}^n - R_j{}^n)\cdot A = \rho_0 \cdot \Delta x \cdot A \tag{5}$$

Dividing by Δx and taking limit as $\Delta x \to 0$

$$(\rho_p + \rho_g)\cdot \partial R/\partial x = \rho_0 \tag{6}$$

Gaseous Specific Volume

$$v_{j+1/2}{}^n = \frac{(R_{j+1}{}^n - R_j{}^n)\cdot A - (M_{pj+1/2}{}^n/\rho_1)}{M_{gj+1/2}{}^n} \tag{7}$$

Substituting Eq. (4) in Eq. (7) and taking limit as $\Delta x \to 0$

$$v = (\rho_1 - \rho_p)/(\rho_1 \cdot \rho_g) \tag{8}$$

Conservation of Momentum

Equating force to the rate of change of momentum

$$\begin{aligned} A\cdot\{(\rho_{pj+1/2}{}^{n+1} + \rho_{gj+1/2}{}^{n+1})\cdot(R_{j+1}{}^{n+1} - R_j{}^{n+1})\cdot u_{j+1/2}{}^{n+1} - \\ (\rho_{pj+1/2}{}^n + \rho_{gj+1/2}{}^n)\cdot(R_{j+1}{}^n - R_j{}^n)\cdot u_{j+1/2}{}^n\} \\ = -A\cdot\Delta t\cdot(p_{j+1}{}^{n+1/2} - p_j{}^{n+1/2}) \end{aligned} \tag{9}$$

Taking Taylor series expansion about $(n+\frac{1}{2})$, dividing by $\Delta x \Delta t$ and letting $\Delta x, \Delta t \to 0$

$$\partial u/\partial t = -(1/\rho_0)\partial p/\partial x \tag{10}$$

It should be noted that since there is no relative velocity between propellant and gases, whether the matter exists in the solid phase or in the gaseous phase is immaterial so far as momentum is concerned.

Conservation of Energy

The Lagrangean element $(x,x+\Delta x)$ can be considered as a closed system since there is no mass transfer across the boundaries of the element. Also there is no heat transfer across the element boundaries and the first law of thermodynamics can be written as

$$0 = \Delta E + \Delta KE + \Delta PE + \Delta W_1 - \Delta W_2 \tag{11}$$

For small Δx, the closed system can be taken to undergo a quasistatic process and ΔW_1 can be calculated as a product of pressure and change in volume.

$$\begin{aligned} 0 = {} & \{E_{j+1/2}{}^{n+1}\cdot M_{gj+1/2}{}^{n+1} - E_{j+1/2}{}^n \cdot M_{gj+1/2}{}^n\} \\ & + \tfrac{1}{2}\{(M_{gj+1/2}{}^{n+1} + M_{pj+1/2}{}^{n+1})\cdot(u_{j+1/2}{}^{n+1})^2 \\ & \qquad - (M_{gj+1/2}{}^n + M_{pj+1/2}{}^n)\cdot(u_{j+1/2}{}^n)^2\} \\ & + C\cdot\{M_{pj+1/2}{}^{n+1} - M_{pj+1/2}{}^n\} \\ & + p_{j+1/2}{}^{n+1/2}\cdot\{(R_{j+1}{}^{n+1} - R_j{}^{n+1}) - (R_{j+1}{}^n - R_j{}^n)\}\cdot A \\ & - A\cdot\tfrac{1}{2}\{p_j{}^{n+1/2} - p_{j+1}{}^{n+1/2}\}\cdot\{R_j{}^{n+1} - R_j{}^n + R_{j+1}{}^{n+1} \\ & \qquad - R_{j+1}{}^n\} \end{aligned} \tag{12}$$

It should be noted that $\Delta KE = \Delta W_2$. Taking Taylor series expansion about n, dividing by $\Delta x \Delta t$ and letting $\Delta x, \Delta t \to 0$

$$\partial/\partial t\{\partial R/\partial x\cdot(E\cdot\rho_g + C\cdot\rho_p)\} = -p\cdot\partial/\partial t\{\rho_0/\rho_p + \rho_g\} \tag{13}$$

Equation of State

$$p\cdot(v-\eta) = R_0\cdot T \tag{14}$$

Since the gases are polytropic with constant specific heats

$$E = C_v \cdot T$$

$$R_0 = C_p - C_v$$

Hence

$$E = p \cdot (v - \eta)/(\gamma - 1) \tag{15}$$

Burning Rate Equation

The relationship between mass burning rate and the radial burning rate can be obtained as follows:

$$M_{pj+1/2}{}^{n+1} - M_{pj+1/2}{}^{n} = \tfrac{4}{3} \cdot \pi \cdot \{(r_{j+1/2}{}^{n+1})^3 - (r_{j+1/2}{}^{n})^3\} \cdot n_1 \rho_1 \Delta x/L \tag{16}$$

Dividing both sides by $\Delta x \cdot \Delta t$ and taking limit as $\Delta x, \Delta t \to 0$

$$\frac{\partial m_p}{\partial t} = \frac{4 \cdot \pi \cdot n_1 \cdot \rho_1}{V_c} \cdot r^2 \cdot \frac{\partial r}{\partial t} \tag{17}$$

where $m_p = \rho_p \cdot (\partial R/\partial x)$. In the following $\partial m_p/\partial t$ and $\partial r/\partial t$ are referred to as the mass burning rate and the radial burning rate, respectively.

Initial Conditions

At $t = 0$, for all x,

$$u = 0$$

$$p = \text{pressure produced by primer} \tag{18}$$

$$v = \text{specific volume due to air and primer gases}$$

Boundary Conditions

At breech, $u = 0$ for all t. At projectile base, the equation of motion is given by

$$d^2R_b/dt^2 = [(p_b - p_a)/m] \cdot A \qquad p_b > p_{\min} \tag{19a}$$

otherwise,

$$u_b = 0 \qquad p_b \leq p_{\min} \tag{19b}$$

Finite Difference Scheme

The differential equations are first nondimensionalized with respect to reference length L_0, specific volume v_0 and pressure p_0 so that the same set of equations can be used with any system of units. Nondimensionalization does not change the form of the equations and the same symbols have been used to denote nondimensionalized quantities.

The momentum equation and the equation of state can be written in the difference form as

$$\frac{u_j{}^{n+1/2} - u_j{}^{n-1/2}}{\Delta t} = -\frac{1}{\rho_0} \cdot \frac{p_{j+1/2}{}^{n} - p_{j-1/2}{}^{n}}{\Delta x} \tag{20}$$

and

$$E_{j+1/2}{}^{n+1} = \frac{p_{j+1/2}{}^{n+1} \cdot (v_{j+1/2}{}^{n+1} - \eta)}{\gamma - 1} \tag{21}$$

Equations (1, 3, 7, 12, 16, 20, and 21) form a difference scheme of order of accuracy $0(\Delta x)^2 + 0(\Delta t)^2$. The initial conditions are given in Eq. (18) and the equation of projectile motion is

$$m \cdot (R_b{}^{n+1} - 2R_b{}^{n} + R_b{}^{n-1}) = \Delta t^2 \cdot (p_b - p_a) \cdot A \tag{22}$$

For numerical solution of the difference scheme, at $t = 0$, the space behind the projectile is divided into equal elements of width Δx and subsequent evaluations are made at time intervals Δt.

Table 1 Characteristics of Charge, Projectile and Weapon

Charge (unrolled nitrocellulose particles)	
Primer energy	= 9.14 cal.
Charge weight	= 19 grains
Initial temperature of charge	= 70°F
Mean particle diameter	= 0.0263 in.
Calorific value of charge	= 900 cal/g
Density of charge	= 1.55 g/cm^3
Initial mass of air in chamber	= 26.26 × 10^{-7} lbm
Covolume	= 32.2 in.^{3}/lb
Ratio of specific heats	= 1.25
Projectile	
Projectile mass	= 0.00787 lbm
Weapon	
Bore diameter	= 5.56 mm
Chamber volume	= 0.1088 in.^{3}
Barrel length beyond chamber	= 18.5 in.
Minimum pressure for projectile motion	= 2530 psi
Pressure ahead of the projectile	= 14.7 psi

The difference scheme is implicit and to simplify calculations the continuous burning of charge is considered as a large number of instantaneous burning steps equispaced at time interval Δt. To ensure stability of this numerical scheme, Δt must satisfy the following inequality

$$\Delta t \leq \Delta x \cdot \{(v - \eta)/(\gamma \cdot p \cdot v^2)\}^{1/2} \cdot \{\rho_0/(\rho_p + \rho_g)\} \tag{23}$$

Fifteen fluid elements with Δt equal to 0.00267 ms. yielded a stable numerical scheme.

Empirical-Mechanistic Iterative Model Building

Once the characteristics of propellant, projectile and weapon are specified, as shown in Table 1, the only unknown quantity in the formulated model is the mass burning rate $\partial m_p/\partial t$. The present model building consists of obtaining an expression for the mass burning rate which can predict the experimentally observed interior ballistic phenomena. As many different responses (experimental data) as possible should be employed to build a model. Presently, only one such response, namely, the experimental chamber pressure-time curve is considered and the iterative model building approach is used to arrive at a burning rate equation that would closely predict this response. It is hoped that other responses, such as base pressure, velocity, etc., will be predicted reasonably well.

Iterative Model Building

Physical systems can be modeled along three broad categories: mechanistic, empirical-mechanistic and empirical. The particular choice of model class depends upon the present degree of knowledge about the system and the objectives of the analysis. A mechanistic model based on extensive knowledge has the advantage of meaningful extrapolation and physical interpretation. An empirical approach is necessary when very little is known about the system. Since the interior ballistic mechanism is partially understood, an empirical-mechanistic approach is followed.

The iterative model building approach[8,9] is diagramatically shown in Fig. 2. Model building begins by an initial formulation of the model. The formulated model contains unknown parameters which are estimated for best fit to the data. Model is then diagnostically checked for adequacy of fit. Diagnostic checks indicate the nature and possible causes

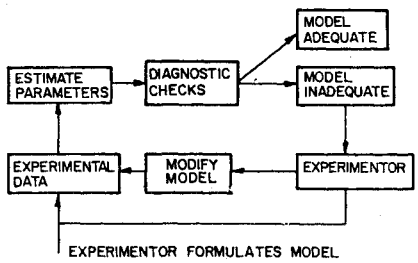

Fig. 2 Model building cycle.

of model inadequacy. A theoretical or experimental investigation of these possible reasons for model inadequacy would indicate the appropriate model corrections to be made. Such an iterative approach will ultimately lead to an adequate model within the region of experimentation.

Experimental Setup and Results

A piezoelectric gage was mounted at midchamber position (point A in Fig. 1) and the pressure-time history was recorded for each round. Muzzle velocity was computed by measuring the time taken by the projectile to travel between two magnetic screens placed known distance apart. Five rounds were fired using charge weight, mean particle diameter and initial temperature of charge as specified in Table 1. The observed pressure-time curves are given in Fig. 3 (dotted curves) and the corresponding muzzle velocities are: 2045, 2092, 2091, 2081, and 2088 ft/sec, respectively.

Stages of Iteration

Four stages of interation are presented to obtain a burning rate model that reasonably explains the observed pressure-time curves. The final form of the burning rate model is known,[10] however, these stages serve to illustrate the interative model building procedure.

Stage 1

It was first assumed that the charge burns completely before the projectile starts to move (instantaneous burning). The resulting chamber pressure was calculated from the equation of state as 46.86×10^4 psi. This pressure is about twenty times the maximum pressure encountered in the experiment, suggesting a finite burning rate.

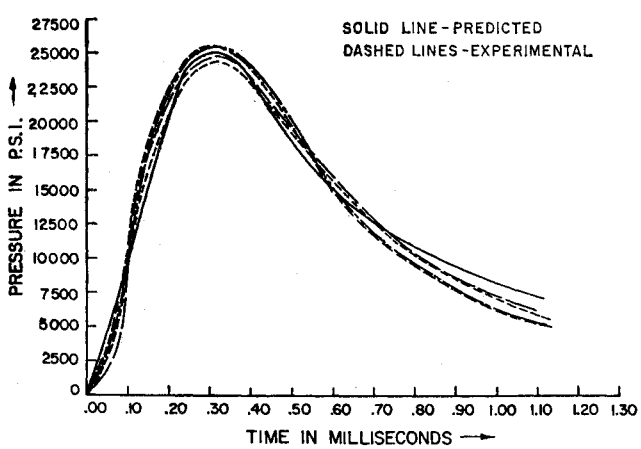

Fig. 3 Experimental and predicted pressure-time curves.

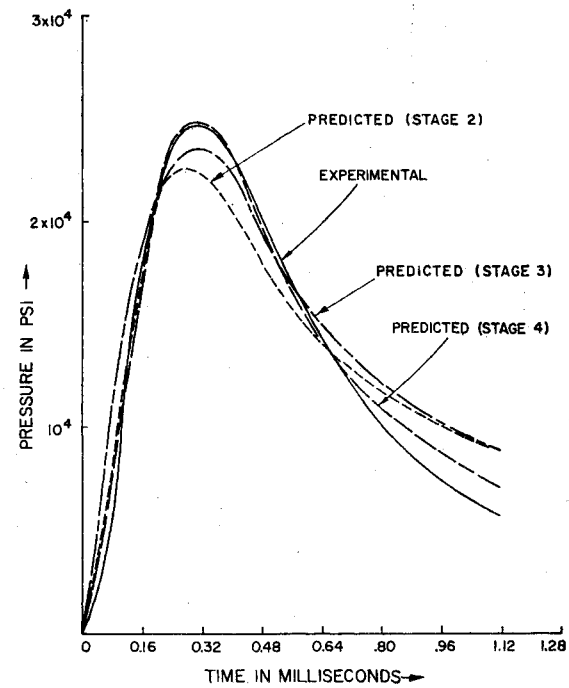

Fig. 4 Iterative model building.

Stage 2

Next assumption was one of uniform burning rate, namely, $\partial m_p/\partial t = K_1$ for all j and n. The constant was estimated from the data using a nonlinear least squares method. For estimation, the five experimental pressure-time curves were discretized by taking 29 equispaced observations from each curve after eliminating ignition delay. The estimation criterion (Appendix) is to find the value of K_1 $(=\hat{K}_1)$ that minimizes the sum of squares of residuals

$$SS(K_1) = \sum_{l=1}^{5} \sum_{m=1}^{29} (p_{lm} - \hat{p}_{lm})^2$$

where p_{lm} is the mth observation on the lth curve and $\hat{p}_{lm}$ is the corresponding predicted pressure. $\hat{K}_1$ was found to be 1.5×10^3 which implies that the entire propellant burns in 1.55 ms.

Figure 4 shows the experimental curve, which is the average of the five experimental pressure-time curves of Fig. 3, and the fitted curve. The minimum sum of squares is found to be 775.3×10^6 (psi)^2. The fitted curve is similar in appearance to the experimental curve, however, the predicted pressures are too large in the initial portions of the curve and are too low near the peak. This discrepancy suggested that the mass burning rate should be small where pressures are small and should be large where pressures are large. In other words, mass burning rate should be considered as a monotonically increasing function of the surrounding pressure.

Stage 3

A study of the burning characteristics of the propellant revealed that as the pressure increases, the flame zone is pushed near the propellant particles leading to a higher heat transfer into the particles and a faster rate of burning. The following functional relationship was assumed for the mass burning rate

$$\partial m_p/\partial t = K_1 \cdot pK_2$$

Nonlinear estimation of K_1 and K_2 gives $\hat{K}_1 = 0.845$, $\hat{K}_2 = 0.196$ and $SS(\hat{K}_1, \hat{K}_2) = 544 \times 10^6$ (psi)^2. The fitted pressure-time curve is shown in Fig. 4. Compared to the

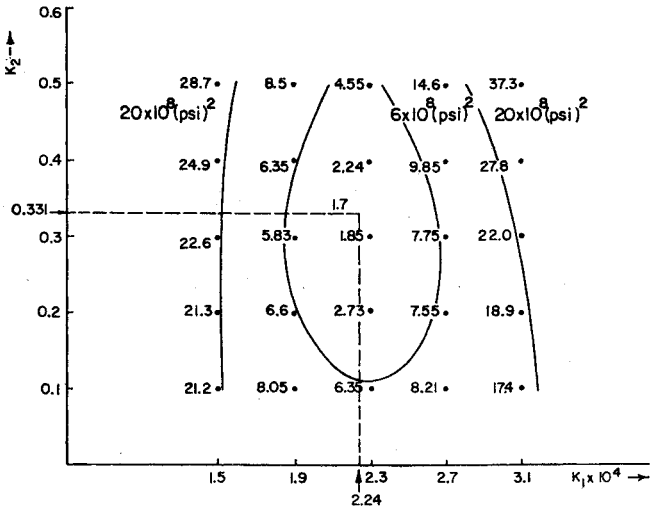

Fig. 5 Sum of squares contours.

predicted pressure-time curve at stage 2, this curve is closer to the experimental one, as seen from the reduced sum of squares of residuals.

There are two sources of discrepancy. The predicted pressures are lower near the peak and higher toward the end of the pressure-time curve. The requirement of lower pressures in the later portion of the curve suggested the following modification. As burning proceeds, the available burning surface area reduces, thereby reducing the rate of mass burning. Therefore, mass burning rate (as differentiated from radial burning rate) should be taken as a function of the burning surface area. This would result in smaller pressures toward the end of the curve. The estimation procedure would lead to increased burning rate. The net result would be an increase in the predicted peak pressure and a reduction in predicted pressures toward the later portion of the curve.

Stage 4

It was now assumed that

$$\partial m_p/\partial t = S \cdot K_1' \cdot pK_2$$

But from Eq. (17)

$$\partial M_p/\partial t = S \cdot (n_1/V_c) \cdot \rho_1 \cdot (\partial r/\partial t)$$

The model was therefore taken to be

$$\partial r/\partial t = K_1 \cdot pK_2$$

where $K_1 = (\rho_1 \cdot n_1/V_c) \cdot K_1'$. The estimated constants are $\hat{K}_1 = 2.24 \times 10^{-4}$, $\hat{K}_2 = 0.331$ and $SS(\hat{K}_1,\hat{K}_2) = 169.5 \times 10^6$ (psi)^2.

The predicted pressure-time curve is shown in Fig. 4 and in Fig. 3 (solid line). The model at this stage is seen to predict the observed data reasonably well. Figure 5 is a plot of the sum of squares of residuals for different values of K_1 and K_2. The sum of squares surface is found to be well-behaved and the contours of constant sum of squares indicate that the estimated parameter values correspond to the minimum in the plotted region.

$\hat{K}_1$ and $\hat{K}_2$ may be considerably different from the burning rate constants obtained from closed bomb experiments because factors such as ignition delay, erosive burning, heat transfer, friction, etc., have not been explicitly considered. The estimated constants may be deemed as adjusted burning rate constants which tend to account for the model assumptions.

Analysis of Predicted Ballistic Phenomena

The purpose of this analysis is threefold: to understand the implications of the basic assumptions of the model, to gain

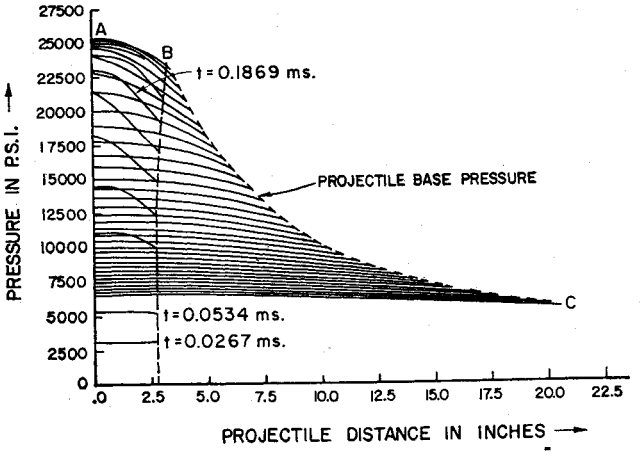

Fig. 6 Pressure variation along barrel.

a qualitative understanding of the ballistic phenomena to be expected in practice, and to serve as a diagnostic check on the model. The model with estimated parameter values was used to numerically evaluate the special case of 5.56 mm weapon with characteristics specified in Table 1. The results are shown in Figs. 6–10.

Figure 6 shows the variation of pressure in the space behind the projectile for successive positions (0.0267 ms. apart) of the projectile along the barrel. The fan of rarefaction waves moving toward the breech end and its successive reflections at the breech and at the projectile base can be observed from the figure. At all times a nonincreasing pressure gradient exists between the breech and the projectile base. The ratio of base to breech pressure, shown in Fig. 7, oscillates and tends to stabilize about its mean value of 0.85 which is close to the value predicted by Pidduck's limiting solution.[2] The points of minima and maxima in Fig. 7 correspond to the wave reflections at the breech and at the base respectively. Under the present set of assumptions, no support is lent to the theory, apparently favoured by Charbonnier as reported in Pidduck,[2] of more or less violent impulses of pressure on the projectile base.

Figure 6 also shows the variation of projectile base pressure (dotted curve) and the variation of the maximum pressure (curve ABC) as a function of distance along the barrel. The maximum pressure curve is of interest in barrel design.

Figure 8 shows the particle path for different starting positions of the particles. For any t, the ratio $R(x,t)/R(x,0)$ remains approximately constant for all x. Figure 9 shows the variation of fluid velocity behind the projectile. The velocity

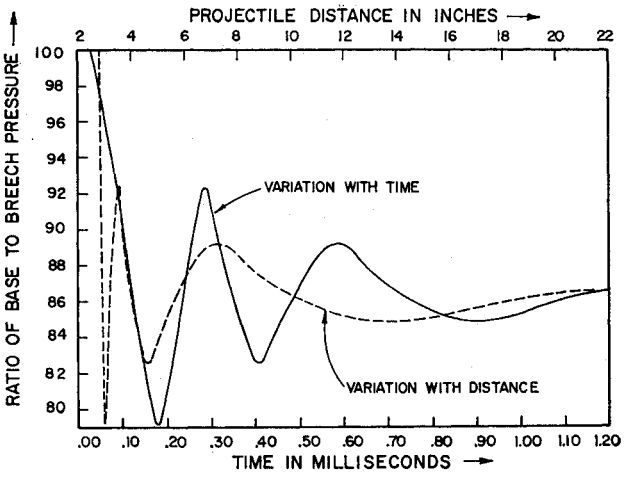

Fig. 7 Ratio of base to breech pressures.

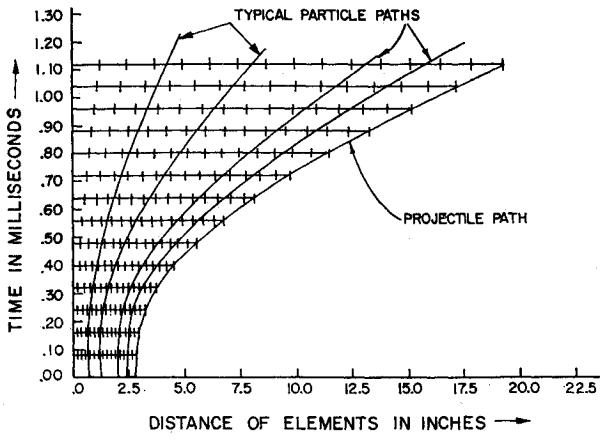

Fig. 8 Time variation of element positions.

variation from breech to base, at any t, is approximately linear. Therefore, the assumption of linear velocity variation from breech to base, first introduced by Lagrange and used in many classical interior ballistic theories, appears to be satisfactory. Figure 10 shows the time variation of projectile distance, velocity and acceleration. The predicted muzzle velocity of 2250 ft/sec is about 9% higher than the average observed muzzle velocity of 2079 ft/sec.

Finally, the model predicts that the total energy of propellant and primer is distributed as internal energy of gases (43.5%), kinetic energy of projectile (18.3%), kinetic energy of gases (2.2%), and potential energy of unburnt propellant (36%). The predicted unburnt propellant and higher muzzle velocity necessitate a review of the basic model assumptions. Such a review suggests different possibilities for model improvement, the incorporation of heat transfer, friction and the relative velocity between propellant and gases being the most probable ones.

Conclusions

1) One-dimensional Lagrangean differential and difference equations are derived for the practical case of two phase flow in the weapon. The differential equations constitute the formulated model with the burning rate equation being the only unknown quantity.

2) For the case of 5.56 mm weapon using nitrocellulose charge, the iterative model building technique is successfully employed to arrive at a burning rate equation that predicts the observed pressure-time curves reasonably well.

3) Numerical evaluation of the model gives a qualitative understanding of the interior ballistic phenomena to be

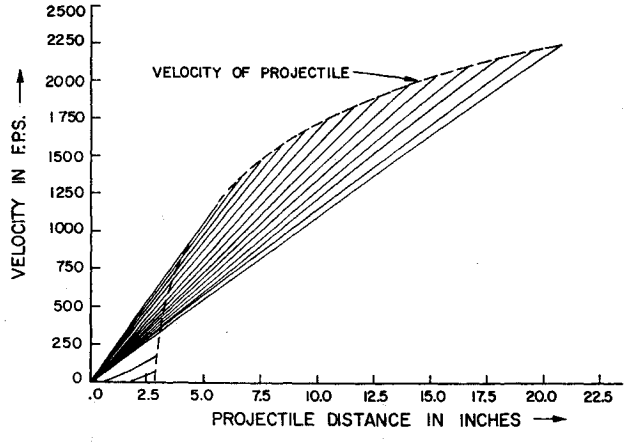

Fig. 9 Velocity variation along barrel.

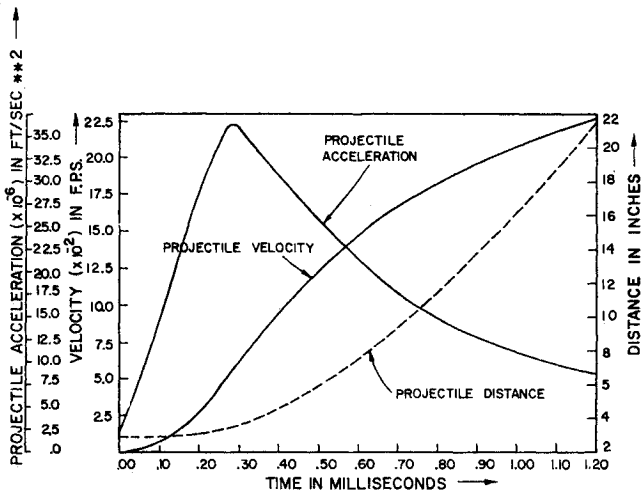

Fig. 10 Projectile distance, velocity and acceleration.

expected in practice. It also serves as a diagnostic tool and shows that better prediction of velocity is likely to be obtained if heat transfer and friction are taken into account.

Appendix: Parameter Estimation

The procedure to obtain least squares estimates of the burning rate parameters K_1 and K_2 using Marquardt's[11] method is explained. Actual calculations were performed using the computer program "NREG"[11] and the subroutine "MODEL" which is a computer program to solve the difference scheme.

The model for the continuous pressure-time curve can be written as

$$p(t) = f(K_1,K_2,\xi,t) + \varepsilon(t)$$

Here $p(t)$ is the chamber pressure and $\varepsilon(t)$ is the error. $f(K_1,K_2,\xi,t)$ is the response function that predicts the chamber pressure for given values of the burning rate parameters and the experimental conditions ξ. The model is nonlinear in parameters and the response function is implicit.

For the given experimental data, the discrete model can be written as

$$p_t^{(l)} = f(K_1,K_2,\xi,t) + \varepsilon_t^{(l)} \qquad \begin{matrix} t = 1,2,\ldots,29 \\ l = 1,2,\ldots,5 \end{matrix}$$

or in matrix form

$$P = F + \varepsilon$$

where all the three matrices are 145×1.

Step 1: Obtain initial values for parameters to start the iterative estimation procedure. Initial value of K_2 can be taken to be between 0 and 1 and the order of magnitude of K_1 can be obtained by a consideration of the burning rate equation and the approximate time for complete burning. Let the initial parameter values be

$$K^{(0)} = \begin{bmatrix} K_1^{(0)} \\ K_2^{(0)} \end{bmatrix}$$

Step 2: Set up a derivative matrix Z. Each element of this matrix is calculated from

$$z_{it}^{(l)} = \left.\frac{\partial f(K_1,K_2,\xi,t)}{\partial K_i}\right|_{K=K^{(0)}} \qquad \begin{matrix} i = 1,2 \\ t = 1,2,\ldots,29 \\ l = 1,2,\ldots,5 \end{matrix}$$

Since the functional relationship is implicit, the derivatives are numerically evaluated. Same value of derivative will be obtained for each of the five replicated observations at a given time point.

Step 3: Obtain $Z'Z$ and scaled matrix D

$$B = Z'Z = \begin{bmatrix} b_{11} & b_{12} \\ b_{12} & b_{12} \end{bmatrix}$$

The scale factors are

$$C_{11} = (b_{11})^{1/2}$$
$$C_{22} = (b_{22})^{1/2}$$

and each element of matrix D is given by

$$d_{ij} = b_{ij}/(C_{ii}C_{jj})^{1/2} \qquad \begin{matrix} i = 1,2 \\ j = 1,2 \end{matrix}$$

Step 4: Calculate $Z'(P - F_0)$ and scaled matrix G. F_0 is the response function matrix F evaluated at $K = K^{(0)}$. The scaled matrix G is obtained by dividing each element of $Z'(P - F_0)$ by square root of the scale factor.

Step 5: Set up the equation

$$(D + \lambda I)\delta^* = G$$

where λ is a constant (0.01) and solve for δ^*

$$\delta^* = (D + \lambda I)^{-1}G = \begin{bmatrix} \delta_1^* \\ \delta_2^* \end{bmatrix}$$

Step 6: The new parameter estimates are

$$K_1^{(1)} = K_1^{(0)} + \delta_1^*$$
$$K_2^{(1)} = K_2^{(0)} + \delta_2^*$$

Step 7: Iterate with proper λ till convergence occurs.[11] The convergence criterion is

$$\left| \frac{SS(K^{(i)}) - SS(K^{(i-1)})}{SS(K^{(i-1)})} \right| \leq 10^{-5}$$

where $SS(K^{(i)})$ is the sum of squares of residuals at the end of the ith iteration and $SS(K^{(i-1)})$ is the sum of squares of residuals at the end of the $(i-1)$th iteration.

References

[1] Poisson, M. C., "Mouvement de Poulet dans L'Interieur de Canon," Extraites des Manuscripts de Lagrange, *Journal d'Ecole Polytech*, Vol. 21, 1832, p. 13.

[2] Love, A. E. H. and Pidduck, F. D. B., "Lagrange's Ballistic Problem," *Philosophical Transactions of the Royal Society*, Vol. 222, 1922, pp. 167–226.

[3] Heybey, W., "A Solution of Lagrange's Problem by Means of Characteristic Lines," Memo 10819, 1950, U.S. Naval Ordnance Lab., Md.

[4] Carriere, P., "The Method of Characteristics Applied to the Problems of Internal Ballistics," *Proceedings of the 7th International Congress of Applied Mechanics*, Vol. 3, 1948, pp. 139–153.

[5] Haden, M. G., "Numerical Solution of the Lagrange Ballistic Problem During the Burning of the Charge," ARDE Memo 10/61, 1961.

[6] Murphy, J. R. B., Badhwar, L. K., and Lavoie, G. A., "Interior Ballistics Calculation Systems for Light Gas Guns and Conventional Guns," *AGARD Conference Proceedings*, No. 10, 1966, pp. 51–78.

[7] Richtmyer, R. D. and Morton, K. W., *Difference Methods for Initial Value Problems*, Interscience Publishers, New York, 1967, Chap. 12.

[8] Box, G. E. P. and Hunter, W. G., "A Useful Method for Model Building," *Technometrics*, Vol. 4, No. 3, 1962, pp. 301–318.

[9] Saxena, U. K. and Wu, S. M., "Building a Mathematical Model to Predict Transient Drilling Temperature Responses," *Transactions of the ASME, Journal of Engineering For Industry*, Vol. 91, 1969, pp. 641–651.

[10] Corner, J., *Theory of Interior Ballistics of Guns*, Wiley, New York, 1950, Chap. 2.

[11] Ryshpan, J., "Nonlinear Regression Routine," 1972, Academic Computing Center, University of Wisconsin, Madison, Wis.